Investigating protein-protein interactions in living cells using fluorescence lifetime imaging microscopy

Yuansheng Sun[1], Richard N Day[2] & Ammasi Periasamy[1]

[1]W.M. Keck Center for Cellular Imaging, Departments of Biology and Biomedical Engineering, University of Virginia, Charlottesville, Virginia, USA. [2]Department of Cellular and Integrative Physiology, Indiana University School of Medicine, Indianapolis, Indiana, USA. Correspondence should be addressed to A.P. (ap3t@virginia.edu).

Published online 11 August 2011; doi:10.1038/nprot.2011.364

Fluorescence lifetime imaging microscopy (FLIM) is now routinely used for dynamic measurements of signaling events inside living cells, including detection of protein-protein interactions. An understanding of the basic physics of fluorescence lifetime measurements is required to use this technique. In this protocol, we describe both the time-correlated single photon counting and the frequency-domain methods for FLIM data acquisition and analysis. We describe calibration of both FLIM systems, and demonstrate how they are used to measure the quenched donor fluorescence lifetime that results from Förster resonance energy transfer (FRET). We then show how the FLIM-FRET methods are used to detect the dimerization of the transcription factor CCAAT/enhancer binding protein-α in live mouse pituitary cell nuclei. Notably, the factors required for accurate determination and reproducibility of lifetime measurements are described. With either method, the entire protocol including specimen preparation, imaging and data analysis takes ~2 d.

INTRODUCTION

Fluorescence lifetime is the average time that a molecule spends in the excited state before returning to the ground state, typically with the emission of a photon. The fluorescence lifetime of a fluorophore (in the absence of nonradiative processes) is an intrinsic property of the fluorophore, and it carries information regarding events in the probe's local microenvironment that affect the photophysical processes[1,2]. Fluorescence lifetime was first measured in 1870 from phosphorescence (or delayed fluorescence)[3]. The first nanosecond-lifetime measurements using optical microscopy were made in 1959 (ref. 4). Since then, numerous fluorescence lifetime imaging microscopy (FLIM) methodologies have evolved for various biological and clinical applications[5] (also see Chapter 22 in ref. 1).

As the lifetime of a fluorescent molecule is sensitive to its local microenvironment, cellular responses to events such as changes in temperature, pH and ion (e.g., calcium) concentrations can be measured very accurately using FLIM[6,7]. For example, FLIM was applied to detect the free (short lifetime) and bound (long lifetime) forms of NADH (a convenient noninvasive fluorescent probe of the metabolic state)[8], showing promise in cancer research[9]. FLIM was also used to study dental disease through imaging endogenous fluorophores in dental tissues[10], and multiphoton FLIM tomography (3D lifetime distribution) of human skin was used to distinguish between different types of endogenous fluorophores[11]. In addition, multiphoton multispectral FLIM has the potential to become a valuable technique in stem cell research[12]. The presenilin 1 protein is associated with Alzheimer's disease (AD). FLIM was implemented to investigate different conformational changes of the presenilin 1 protein and the study provided further understanding of the AD diagnosis[13]. FLIM techniques were also applied in plant biology. Eckert *et al.*[14,15] used the wide-field single photon counting FLIM technique to investigate the fluorescence dynamics of the chlorophyll d-containing cyanobacteria *Acaryochloris marina*.

An important application of FLIM is the measurement of FRET between fluorescent molecules[16–27]. FRET is the nonradiative transfer of excited-state energy from one molecule (the donor) to another nearby molecule (the acceptor) via a long-range dipole-dipole coupling mechanism[28,29]. As the efficiency of energy transfer from the donor to the acceptor is dependent on the inverse of the sixth power of the distance separating them (see Chapter 13 in ref. 1), FRET is usually limited to distances less than ~10 nm, and thus provides a sensitive tool for investigating a variety of phenomena that produce changes in molecular proximity[30–33]. Because energy transfer is a quenching process that depopulates the excited state of the donor fluorophore, the donor fluorescence lifetime is shortened by FRET. FLIM maps the spatial distribution of probe lifetimes inside living cells, and can accurately measure the shorter donor lifetimes that result from FRET[26,34].

We have previously published a protocol for FLIM measurements using the gated image intensifier[35]. In this current report, we describe in detail the procedures that are necessary to use both a time-domain (TD) FLIM method and a frequency-domain (FD) FLIM method to monitor protein-protein interactions in live specimens based on FRET. These methods are routinely used in our laboratories for a variety of FRET applications[17,20,22,23,26,27,31,36–44]. The biological case chosen for demonstration is the dimerization of the transcription factor CCAAT/enhancer binding protein-α (C/EBPα) in live mouse pituitary cell nuclei[20,45]. Here the live-cell measurements were made using two commercially available FLIM systems—the Becker & Hickl (BH) time-correlated single-photon counting (TCSPC) FLIM system (TD method) and the ISS ALBA FastFLIM system (FD method). It should be noted that we are not comparing the two FLIM methods (see ref. 46 for a comparison), which work equally well in our case. The sole purpose of this report is to provide the basic procedures that are necessary for successful measurements using both methods, allowing the readers to conduct experiments using the FLIM method that is appropriate for their own biological investigations. The methodology described here can be adapted for other commercial one-photon or two-photon FLIM systems.

Overview of FLIM measurements

A typical FLIM experiment involves four steps: (i) calibrate the FLIM system with fluorescence lifetime standards; (ii) acquire FLIM data from biological specimens; (iii) analyze the data to extract lifetime information; and (iv) interpret the analyzed data to illustrate the biological activity or other experimental objectives. For a FRET study using a FLIM system, the second step usually requires the acquisition of FLIM data from specimens that only have donor fluorophores and specimens containing both donor and acceptor fluorophores.

FLIM instrumentation. The measurement techniques in FLIM are generally subdivided into the TD and the FD methods. The basic physics that underlie the two methods is essentially identical, as both TD and FD are finite Fourier transforms of each other[2]. The TD method uses a pulsed light source synchronized to high-speed detectors and electronics, to measure the fluorescence decay profile at different time windows after each excitation pulse. The fluorescence lifetime is estimated by analyzing the recorded decay profile. The FD method uses a modulated light source to excite a fluorophore, and measures the modulation and phase of the emission signals with a detector modulated at the same frequency as the excitation light (homodyne methods), or a frequency slightly (a few hundred to a few thousands hertz) different from the excitation light (heterodyne methods). In a recent development, called digital FD[47], the detectors are not modulated in reference to the frequency of the excitation light, thus allowing for the acquisition of the entire fluorescence signal. The fundamental modulation frequency is chosen depending on the lifetime of the fluorophore (MHz for nanosecond decays). The phase shift(s) and amplitude attenuation(s) of the emission signal relative to the excitation source are analyzed to estimate the fluorescence lifetime.

Both TD and FD FLIM techniques are now available for acquiring FLIM images in wide-field[48,49] or scanning[46,50] mode, which can provide 3D[51,52] and even spectral[19,24,25,53] information (also see ref. 26). The early FLIM systems were expensive and primarily custom built in biophysics laboratories. In the last 10 years, commercial FLIM systems have become available from companies, including Becker & Hickl (http://www.becker-hickl.de/), Picoquant (http://www.picoquant.com/), ISS (http://www.iss.com/), Intelligent Imaging Innovations (http://www.intelligent-imaging.com/), Lambert Instruments (http://www.lambert-instruments.com/) and Horiba Scientific (http://www.horiba.com/scientific/). These systems can be stand alone or integrated with existing multiphoton, confocal or wide-field microscopy systems for various life-science applications.

Calibration of a FLIM system. Before any biological imaging, an FLIM system must be calibrated with fluorescence lifetime standards. Many standard fluorophores are available for this purpose[54] (also see Appendix II in ref. 1 and an online source at http://www.iss.com/resources/reference/data_tables). Although the calibration procedures vary depending on the setup of the FLIM system, it is important to use a standard fluorophore, the excitation, emission and fluorescence lifetime properties of which are close to those of the fluorophore to be measured in the intended samples. As the fluorescence lifetime of a fluorophore is sensitive to its environment, it is critical to prepare the standard according to the conditions, such as solvent, pH, temperature and optical configuration, specified in the literature.

FLIM data analysis. An intrinsic fluorescence decay $f(t)$ composed of N ($N \geq 1$) fluorescent species is often modeled as a monoexponential ($N = 1$) or multiexponential ($N > 1$) time course in equation (1), where f_0 is the number of total initial photon counts; a_n (often termed as the pre-exponential factor) represents the percentage of the initial photon counts from a fluorescent species with its lifetime τ_n over the total initial photon counts (f_0). For a multiexponential case, the sum of a_1, a_2, … and a_N is usually set as 1, and the apparent lifetime (τ_a) calculated by equation (2) is often used to indicate the mean lifetime of all fluorescent species. Regardless of the FLIM method used, the purpose of the FLIM data analysis is to extract the lifetime components and the associated pre-exponential factors from measured data.

$$f(t) = f_0 \sum_{n=1}^{N} \left\{ a_n \exp\left(-\frac{t}{\tau_n} \right) \right\} \quad (1)$$

$$\tau_a = \sum_{n=1}^{N} (a_n \tau_n), \quad \sum_{n=1}^{N} a_n = 1 \quad (2)$$

A variety of computer algorithms have been developed for FLIM data analysis[26] (also see Chapters 4 and 5 in ref. 1). Some are associated with specific FLIM data acquisition methods. For example, the rapid lifetime determination algorithm is used to analyze time-resolved images acquired by a gating camera[48,55]. However, there are a number of strategies used for both TD and FD FLIM data analysis[26]. For instance, the phasor plot (also termed as AB plot[56] or polar plot[57]), approach that was originally developed for displaying and analyzing FD FLIM data, was recently adapted for TD FLIM data analysis[58]. Some FLIM data analysis strategies vary depending on the particular biological models. For example, the global analysis[59,60] can significantly improve the signal-to-noise ratio in FLIM images, but the method requires an assumption that identical fluorescence relaxation parameters pertain to the pixels grouped together for fitting, which may not be valid in many experimental systems. Fortunately, the commercial software packages for FLIM data analysis continue to evolve, and have become user-friendly tools that process and display fluorescence lifetimes for each pixel in an image.

Assessment of FLIM results. Investigating and assessing the accuracy of the fluorescence lifetime measurements acquired from specimens can be challenging. In particular, determining accurate values of all the nanosecond-scale lifetime components from a multiexponential decay (e.g., $N > 1$ in equation (1)) can be difficult, and most probes will have multiexponential decays inside living systems. Most FLIM data analysis routines involve fitting of the measured data based on a chosen exponential model defined by equation (1). The goodness of fit is considered as an important factor for making the decision on whether or not to accept FLIM results, and is usually assessed by the calculated standard weighted least squares (termed as χ^2) and the residuals, as well as by visually comparing the fitting curve versus the measured data points. The value of χ^2, indicating a good fit for an appropriate model and a random noise distribution, should be close to 1, as predicted by Poisson statistics with enough data points for fitting (see Chapters 4 and 5 in ref. 1). In theory, fitting can always be improved with more exponents. This raises a question that often confuses the users: should a more complicated model, e.g.,

from monoexponential to biexponential, be applied? The answer is probably 'yes', if there is a significant drop in χ^2 value or there is a significant improvement in the fit to the data. However, it is usually difficult to define an explicit change in χ^2 that should be considered as a significant drop. One should always be careful when accepting a more complicated model for data analysis, as it is the reproducibility of data for a particular data processing model that is crucial. Most importantly, more photon counts are required to obtain an accurate statistical fit of the lifetime data when resolving more lifetime components.

Interpretation of FLIM-FRET data. As described above, FRET can be identified by measuring the fluorescence lifetimes of the donor in the presence and the absence of the acceptor. A method of quantifying FRET by FLIM is to calculate the energy transfer efficiency (E) based on equation (3) (see Chapter 13 in ref. 1).

$$E = 1 - \frac{\tau_{DA}}{\tau_D} \quad (3)$$

τ_{DA} (the quenched lifetime of the donor) is measured from the specimens containing both the donor and the acceptor, and τ_D (the unquenched lifetime of the donor) is usually determined from the donor-alone specimens. In the majority of FRET measurements, estimation of τ_{DA} requires two-component analysis ($N = 2$ in equation (1)), which yields two species—one with a shorter lifetime τ_1 and the other with a longer lifetime τ_2. In such a case, one may wonder what should be used as τ_{DA} for E calculation, the shorter lifetime (τ_1), the longer lifetime (τ_2) or the mean lifetime of the two species (τ_a) given by equation (2). After careful consideration using the FRET standard constructs as a calibration tool for FRET (described below), we found that using τ_a as τ_{DA} provided better estimation of E, particularly when different FRET methods (intensity-based FRET, TD FLIM-FRET and FD FLIM-FRET) are compared. The same method of E calculation was also used by others[61]. The important point to be considered is the reproducibility of the lifetime and E values for both positive and negative controls of the experiments. To interpret FLIM-FRET results analyzed based on a multiexponential model, one should always examine the distributions of each lifetime component and its associated pre-exponential factor obtained from a large amount of data. The fact that the donor lifetime can be influenced by its local microenvironment must also be considered when comparing the lifetime distributions in different regions of a specimen (e.g., nucleus versus cytoplasm of a cell). As the 'acceptor/donor' ratio influences E in many FRET systems, measuring the acceptor level will certainly help to understand FLIM-FRET data, although it is usually not required for determining E in FLIM-FRET (see ANTICIPATED RESULTS).

Advantages of FLIM over steady-state (intensity-based) microscopy imaging. First of all, FLIM does indeed provide intensity information at very high temporal resolution (down to picoseconds (ps)). As the fluorescence lifetime of a fluorophore is sensitive to its environmental changes, FLIM can be a good choice for visualizing those changes that cannot be revealed by steady-state imaging methods, such as calcium binding, change in pH and so on. Fluorescence lifetime measurements are insensitive to the change in fluorophore concentration, excitation intensity or light scattering, and to some extent of photobleaching; all these factors commonly induce false information in intensity-based imaging. FLIM can help to discriminate the intrinsic fluorescence of a specimen, i.e., autofluorescence[62–65]. The number of fluorophores with different fluorescence lifetimes can be distinguished by FLIM in one imaging channel. As only donor signals are measured for determining E in FLIM-FRET, the method does not usually require the corrections for spectral bleedthrough that are necessary for intensity-based measurements of sensitized emission from the acceptor[22,30,33]. The FLIM-FRET approach has the capability to estimate the percentage of the interacting and non-interacting donor populations, which cannot be distinguished by most of the intensity-based FRET methods. For fluorescence polarization and anisotropy measurements, the FLIM anisotropy decay analysis can often help to differentiate between various causes of depolarization, which usually cannot be directly resolved by steady-state anisotropy imaging[66].

Limitations of FLIM over steady-state (intensity-based) microscopy imaging.

- FLIM is preferably applied to live specimens in life sciences applications, as it can be difficult to distinguish the real fluorescence lifetime changes from those caused by the fixative in fixed specimens.
- Some understanding of the physics of fluorescence lifetime is required for processing the FLIM data and interpretation of the results, particularly for a biological system.
- For FRET applications, it is important to ensure that the donor fluorophores reside in the same microenvironment in both donor-alone control specimens and specimens containing both donor and acceptor fluorophores, as the fluorescence lifetime of a fluorophore can be affected by its microenvironment. A donor molecule, the intrinsic lifetime of which has multiple components, is not suitable for FLIM-FRET, as it will complicate the data analysis.
- As technology improves, the FLIM data acquisition time is expected to decrease. Currently, this time varies from seconds to minutes depending on the setup of a FLIM system (particularly the detector and the specimens to be imaged).

Experimental design

FLIM is technically challenging. To be successful, users should have some understanding of the physics of fluorescence lifetime and the FLIM instrument configuration. An understanding of the required parameters for FLIM data analysis is helpful in interpreting results appropriately because the fluorescence lifetime is sensitive to microenvironmental changes, such as calcium ion concentrations, protein-protein interactions, cancer or AD-related diagnostic parameters. Below we explain the importance of calibrating a FLIM system before using the biological specimen. The explanation provided below is applicable to any FLIM system, either commercially available or custom built.

TCSPC FLIM data acquisition and analysis. TCSPC[67] is the commonly used TD FLIM method. In TCSPC FLIM, the measured data at each pixel, called a decay trace, is composed of photon counts in different time windows relative to the excitation pulse, and can thus be directly plotted over time (nanosecond scale in our case). A measured decay trace is the convolution form of the intrinsic fluorescence decay (see equation (1)) and the instrument response

function (IRF) of the FLIM system. Therefore, an iterative deconvolution algorithm is often used to estimate the lifetime information from the measured data, given a measured or estimated IRF and the choice of exponential model. The criterion for determining the optimal lifetime values is usually based on weighted least-squares numerical approach, in which a fitting curve, generated using the estimated lifetimes and pre-exponential factors, is compared with the measured data.

Measurement of the IRF of the TCSPC FLIM system. Recording the IRF of a TCSPC FLIM system is essential to improve the temporal resolution of the data analysis. The IRF can be estimated from acquired decay data. However, it is preferable to directly measure the IRF experimentally. Generally, an IRF can be measured by recording either the scattered excitation light or the decay of a fast reference dye such as rose Bengal in phosphate buffer, pH 7.4 (lifetime = ~70 ps)[68]. In the first method, for visible light excitation, a strongly scattering specimen such as non-dairy coffee creamer is conventionally used to record the IRF[69]; for infrared light excitation, the IRF can be measured using a sample (such as urea crystal) that yields second-harmonic generation (SHG) signals[70]. SHG is an ultrafast nonlinear process that delivers a signal at one-half of the excitation wavelength. For IRF measurements, it is important to apply the same optics and TCPSC settings used for experimental samples, as the IRF may vary depending on the optical configuration, such as the objective lens. More importantly, the IRF of the TCSPC FLIM system should be periodically checked, as it can change by reflections in the optical path, by poor mode locking of the multiphoton laser or by changing the electronic components such as setting up of constant fraction discriminator and detector parameters.

FD FLIM data acquisition and analysis. In FD FLIM, the measured data at each pixel is usually composed of phase delays (Φ) and amplitude modulation ratios (m), measured at different modulation frequencies (ω). The phase delays increase from 0 to 90 degrees and the modulation ratios decrease from 1 to 0, from low to high frequencies. The lifetime of a single fluorescence species (a monoexponential case) can be directly calculated from either the phase delays by equation (4) (termed as phase lifetime—τ_Φ) or the modulation ratio by equation (5) (termed as modulation lifetime—τ_m), measured at a single frequency. A difference between τ_Φ and τ_m is an indication that the data does not follow a monoexponential time course. For a multiexponential case, the measured phase delays and modulation ratios can be fitted using an exponential model to estimate the lifetime information based on a weighted least-squares numerical approach.

$$\tau_\phi = \tan\Phi/\omega \quad (4)$$

$$\tau_m = \sqrt{1-m^2/(m\omega)} \quad (5)$$

The phasor plot approach mentioned above is usually used in FD FLIM to display and analyze the measured data. Each point representing a pixel in the image will be displayed with a coordinate ($x = m(\omega)\times\cos(\Phi(\omega)), y = m(\omega)\times\sin(\Phi(\omega))$. A semicircle ($(x-0.5)^2 + y^2 = 0.25$) indicates the lifetime trajectory with decreasing lifetime from left to right, where (1, 0) indicates lifetimes near zero to (0, 0) being infinite lifetime. A distribution of points that fall on the semicircle will have only one lifetime component. Conversely, a distribution of points that fall inside the semicircle are likely to have multiple lifetime components.

Calibration of the FLIM systems with reference fluorophores of known lifetime. Prior to any scientific investigation, the FLIM system has to be calibrated with known lifetime fluorescent standards. It is better to select a fluorescence lifetime standard that can be imaged with the same imaging setup used for biological samples. For example, here we use a cyan fluorescent protein—the monomeric Cerulean[71]—as the donor fluorophore; it has a peak absorption wavelength of ~433 nm and a peak emission wavelength of ~475 nm. The fluorescence lifetime of Cerulean in living cells is ~3 ns[61,71]. We used Coumarin 6 dissolved in ethanol (peak excitation and emission wavelengths: 460 nm and 505 nm), with a reference lifetime of ~2.5 ns (http://www.iss.com/resources/reference/data_tables/LifetimeDataFluorophores.html) as a reference to calibrate both our TCSPC and FD FLIM systems, as it allows us to apply the same FLIM setups for our biological specimens. We recommend that the calibration be done every day before the experiment. In FD FLIM, a reference fluorophore of known lifetime is used to establish the excitation profile, and it is essential to input the reference lifetime value into the system software to estimate the lifetime values from experimental data. Besides Coumarin 6 in ethanol, we also used HPTS (8-hydroxypyrene-1,3,6-trisulfonic acid, trisodium salt) dissolved in phosphate buffer pH 7.5 (peak excitation and emission wavelengths: 454 and 511 nm) with an expected lifetime of ~5.3 ns[72] for calibrating our FD FLIM system.

Verification of the FLIM-FRET approach using a FRET-standard genetic construct. Generally, for FRET imaging, it is desirable to use FRET reference standards, in addition to positive and negative controls, to verify the veracity of the FRET results. To this end, a comparative method to determine the accuracy of FRET measurements was developed by the Vogel laboratory (NIH/NIAAA)[61,73]. The approach uses 'standards' in the form of genetic constructs encoding fusions between donor and acceptor fluorescent proteins separated by defined amino acid linker sequences. A genetic construct was generated by encoding Cerulean[71] and Venus[74], directly coupled through the amino acid (aa) linker sequence SGLRS. The expression of the Cerulean-5aa-Venus (C5V) construct results in approximately 43 ± 2% FRET efficiencies[61]. The Cerulean-5aa-Amber (C5A) construct (also designed by the Vogel Laboratory) is used as the donor-alone control. Amber is a nonfluorescent form of Venus, in which a tyrosine was changed to cysteine, thereby producing a protein that folds correctly but that does not function as a FRET acceptor[61]. The C5A protein recapitulates the local environment of the Cerulean donor fluorophore in the C5V FRET standard without the quenching that results from energy transfer. Compared with the C5V construct (positive control), the CTV construct (negative control), in which Cerulean and Venus are separated by a 229-aa linker encoding the TRAF domain, typically provides less than 10% FRET efficiencies[73].

FLIM-FRET to detect dimerization of C/EBPα

The biological model used here is the basic region leucine zipper (bZip) domain of the C/EBPα transcription factor. The bZip family proteins form obligate dimers through their Leu-zipper domains, which positions the basic region residues for binding to

specific DNA elements. Immunocytochemical staining of differentiated mouse adipocyte cells showed that the endogenous C/EBPα protein was preferentially bound to satellite DNA-repeat sequences located in regions of centromeric heterochromatin[75]. When the C/EBPα–bZip domain is expressed as a fusion to the fluorescent proteins (e.g., Cerulean and Venus used here) in cells of mouse origin (such as the pituitary GHFT1 cells used here), it is localized to the well-defined regions of centromeric heterochromatin in the cell nucleus[45,76]. The obligate dimer bound to well-defined structures in the cell nucleus is an ideal tool to test detection of FLIM-FRET.

MATERIALS

REAGENTS

- Urea crystal (Sigma-Aldrich, cat. no. U5128 Urea-ACS reagent, 99.0–100.5%; see REAGENT SETUP)
- Coumarin 6 (Sigma-Aldrich, cat. no. 546283; see REAGENT SETUP)
- HPTS (AnaSpec, cat. no. 84610; see REAGENT SETUP)
- Trypsin-EDTA solution (Fisher Scientific, cat.no. MT25-051-C1)
- F12/DMEM with phenol red and 2.5 mM L-glutamine (ThermoFisher, cat. no. SH30271.01; medium used for general cell culture)
- Newborn calf serum (NBCS) (ThermoFisher, cat. no. SH30118.03)
- F12/DMEM without phenol red, containing 15 mM HEPES (Sigma, cat. no. D206-10x 1L; media used for imaging)
- FuGENE 6 (Roche Applied Science, cat. no. 11814443001)
- Cerulean-5aa-Venus (C5V) construct (provided by S.Vogel at NIH/NIAAA and used for verifying the FLIM-FRET approach on both TCSPC and FD FLIM systems; see **Supplementary Data 1** for the sequence of the C5V plasmid)
- Cerulean-5aa-Amber (C5A) construct (provided by S.Vogel at NIH/NIAAA and used as the donor-alone control for the FRET standard construct (C5V); see **Supplementary Data 2** for the sequence of the C5A plasmid)
- mCerulean C1 vector (provided by M. Davidson at NHMFL of Florida State University and used for generating the Cerulean-bZip construct (see REAGENT SETUP); see **Supplementary Data 3** for the sequence of the mCerulean C1 plasmid)
- mVenus C1 vector (provided by M.Davidson at NHMFL of Florida State University and used for generating the Venus-bZip construct (see REAGENT SETUP); see **Supplementary Data 4** for the sequence of the mVenus C1 plasmid)
- pCDNA His3.1 vector (Invitrogen, cat. no. V38520; see REAGENT SETUP)
- C/EBPα–bZip construct (see REAGENT SETUP)
- Phosphate buffered saline (PBS) (ThermoFisher, cat. no. MT-20-030-CV)
- Dulbecco's calcium- and magnesium-free PBS (ThermoFisher, cat. no. SH30028LS)
- GHFT1 cell line (described in ref. 77; see REAGENT SETUP)
- Nail polish

EQUIPMENT

TCSPC FLIM system

- BH SPC-150 module (Becker & Hickl)
- BH PMC-100-0 photomultiplier tube (PMT; Becker & Hickl)
- BH SPCM software v8.91 (Becker & Hickl)
- BH SPCImage software v2.9.2.2989 (Becker & Hickl)
- Biorad Radiance 2100 confocal/multiphoton imaging system (Carl Zeiss)
- Coherent Verdi pumped Mira 900 tunable mode-locked ultrafast pulsed laser (Coherent)
- Nikon TE300 inverted epifluorescence microscope (Nikon)
- Nikon ×60/1.2 NA water immersion (Nikon)
- Emission filter: HQ 480/40 nm—2p (Chroma Technology, cat. no. NC030887)
- LaserSharp 2000 software (Carl Zeiss)
- Glass cover slips (Fisherbrand, 12-545-102 25CIR.-1)
- Custom-built steel chamber (Note: A commercially available alternative is Invitrogen Attofluor cell chamber, Invitrogen, cat. no. A-7816; details are available at the Invitrogen website)

FD FLIM system

- ISS ALBA FastFLIM system (ISS)
- ISS VistaVision software v4.0.102 (ISS)
- Two avalanche photodiodes (APDs; Micro Photon Devices, PDM series)
- Nichia 5 mW 440 nm pulsed diode laser (Nichia, NDHB510APA)
- Olympus IX71 inverted epifluorescence microscope (Olympus America)
- Olympus ×60/1.2 NA water immersion (Olympus America)
- Semrock FF495-Di02-25-D beam splitter (Semrock, cat. no. 208529)
- Emission filter, 530/43 nm (Chroma Technology, cat. no. 509302)
- Emission filter, ET 480/40 nm (Chroma Technology, cat. no. 224544)
- Chambered cover glass (Thermo Scientific, cat. no. 155379, 155409)

REAGENT SETUP

Urea crystal slide A urea crystal slide is used for measuring the IRF of the TCSPC FLIM system. Sandwich a thin layer of urea crystal (just barely cover the glass surface) between a glass cover slip and a glass slide, and seal the edges with nail polish to avoid the leakage of the urea crystal. Ensure that the same type of glass cover slip is used for cells during imaging. The urea crystal slide can be stored in the refrigerator (4 °C) and reused over a period of years.

Coumarin 6 (50 μM) Coumarin 6 is used to calibrate both the TCSPC and the FD FLIM systems. Dissolve 17.5 mg Coumarin 6 (MW 350.44) per milliliter in 100% (vol/vol) ethanol. The solution is allowed to dissolve overnight at room temperature (22 ± 1 °C). The solution can be stored for months in the refrigerator (4 °C) in a sealed container, protected from light.

HPTS in phosphate buffer (10 mM, pH 7.5) HPTS in phosphate buffer is used for the calibration of the FD FLIM system. Dissolve 5.2 mg of HPTS (MW 524.4) per milliliter in phosphate buffer. The solution can be stored in the refrigerator (4 °C) in a sealed container, protected from light for months. ▲ **CRITICAL** Verify that the pH is 7.5, as during the HPTS lifetime it may change in pH.

C/EBPα–bZip construct Standard recombinant DNA methods can be used to fuse the sequences that code for either Cerulean or Venus into the reading frame of the sequence encoding the rat C/EBPα–bZip domain, starting with the methionine at position 237 (ref. 78). The cDNA encoding the rat C/EBPα is first inserted into the pCDNA His3.1 vector. The sequence encoding the bZip domain is generated by PCR with primers that include the required restriction sites. The product, digested with BspEI and BamHI, is then inserted in-frame into the mCerulean C1 vector to generate the Cerulean-bZip construct (see **Supplementary Data 5** for the plasmid sequence) or the mVenus C1 vector to generate Venus-bZip construct (see **Supplementary Data 6** for the plasmid sequence). All vectors should be confirmed by direct sequencing.

GHFT1 cells GHFT1 cells can be maintained as monolayer cultures in DMEM containing 10% (vol/vol) NBCS at 37 °C in a 5% CO_2 incubator.

Imaging medium (phenol red–free F12) DMEM (1:1) plus 10% (vol/vol) NBCS. The F12/DMEM contains 15 mM HEPES to maintain pH in the absence of 5% CO_2 during imaging. The imaging medium is only used during the imaging course. ▲ **CRITICAL** Phenol red may cause background signals during imaging.

EQUIPMENT SETUP

TCSPC FLIM system The major components required for TCSPC-FLIM are TCSPC boards, a computer, a wide-field or a confocal scanning microscopy unit, a pulsed light source (one- or two-photon), a reference photodiode and a high-sensitivity FLIM detector (PMT or APD). The repetition rate and the pulse width of the pulsed laser should be determined depending on the lifetime values to be measured. For example, the measurement of lifetimes less than 10 ns requires an 80 MHz repletion rate and a pulse width of <150 femtoseconds (fs). It is important to note that the methodology given below using a two-photon excitation laser is the same as that using a one-photon excitation light source. The main difference will be the samples used for measuring IRF (see EXPERIMENTAL DESIGN).

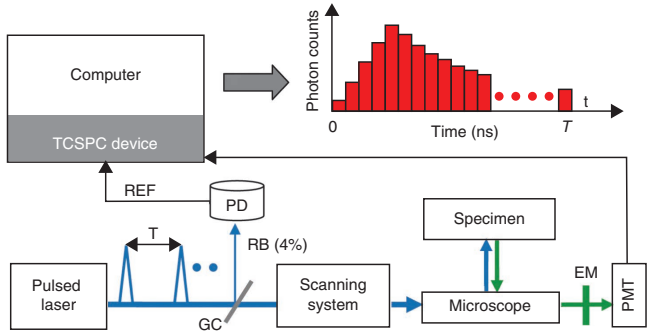

Figure 1 | TCSPC FLIM setup. TCSPC FLIM requires a pulsed excitation source. In our system, a multiphoton laser (repetition rate = 78 MHz, T = 12.82 ns, pulse width <150 fs) is used. The pulsed laser is coupled to the Bio-Rad Radiance 2100 scanning system that is attached to a Nikon TE300 microscope. Thus, spatial information of a specimen is obtained by an *XY* raster scanning mechanism, and is also available in *Z* for optical sections. Photons emitted from the specimen pass through the emission (EM) filter and are detected by a fast detector (timing jitter: 25–300 ps). A photomultiplier tube (PMT) with a response time of ~150 ps is placed in the side port of the microscope (nondescanned detection) and is connected to the TCSPC device. The TCSPC device contains PC plug-in boards (commercially available) that function as the time-to-amplitude converter, time-to-digital converter, discriminator and multichannel analyzer. The TCSPC device synchronizes the detector to the excitation pulse and records the arrival time and spatial information for the detected photons. A reference (REF) signal is acquired from a glass cover slip (GC) reflecting 4% of the excitation light, and this reference beam (RB) is passed to a photodiode (PD) that is connected to the TCSPC device. Given a time period (a few seconds or minutes) of accumulating emitted photons for thousands or millions of excitation pulses, a 'photon counts' histogram is built for each pixel of an image. The fluorescence lifetime at each pixel can be estimated by fitting the corresponding photon counts (decay) data into a single- or multiexponential model.

The setup of our TCSPC FLIM system is illustrated in **Figure 1**, and more detail is available in the literature[20]. The excitation source is a 10 W Verdi pumped, tunable (700–1,000 nm) mode-locked ultrafast (repetition rate =78 MHz) pulsed (pulse width < 150 fs) laser, which is coupled to the laser port of a Bio-Rad Radiance 2100 confocal/multiphoton imaging system. The Bio-Rad system is attached to a Nikon TE300 microscope and controlled by the LaserSharp 2000 software. A specific dichroic mirror (670UVDCLP) equipped on the Bio-Rad system was selected to transmit the multiphoton laser (670–1,000 nm) to scan the specimens through a Nikon ×60/1.2 NA water-immersion objective lens. The photons emitted from the specimens were then reflected by the dichroic mirror to an external fast PMT detector with a response time of ~150 ps. A 480/40-nm band-pass emission filter was placed before the detector. The BH SPC-150 module board is used to allow pixel-by-pixel registration of the accumulated photons. Both the TCSPC FLIM module and PMT detector are controlled by BH SPCM software. A fluorescence decay histogram of photons at different emission times relative to the laser excitation pulse is generated from the distribution of interpulse intervals at each pixel of an image. The recorded decay data are analyzed by the BH SPCImage software to extract lifetime information. The SPCImage software allows users to specify up to three exponential components for fitting, calculates the standard weighted least squares (χ^2) as a quantitative measurement of the fitting significance, and then plots the fitted curve versus the measured decay trace as well as the corresponding residuals for visually assessing the fit. All TCSPC FLIM measurements were carried out at 22 ± 1 °C in a dark room and with a custom-built steel chamber that is used to hold a cover slip containing the specimens.

Measurement of the IRF of the TCSPC FLIM system The IRF of the TCSPC FLIM system was measured by recording the SHG signals from urea crystal (see EXPERIMENTAL DESIGN). We used the 940-nm excitation wavelength and recorded the SHG signals (at 470 nm) with the 480/40-nm emission filter. Although the excitation wavelength (940 nm) used for measuring the IRF is different from that (820 nm) applied to image our biological specimens, the IRF is not influenced by using different excitation wavelengths in our case[43]. This is because the pulse width of the multiphoton laser (<150 fs) is much shorter than the time response of the FLIM detector (~150 ps), which is the main determinant of the full width at half maximum of the IRF.

FD FLIM system The major components required for the FD FLIM system are a light source (continuous wave or pulsed), a modulator, a high quantum efficiency detector (PMT, APD or CCD camera), a computer, a demodulator of the detector or digital image processor and a wide-field or a confocal scanning microscopy unit. In general, the frequency of the modulation of the light source is selected depending on the measurement of the lifetime range. For example, the modulation frequency for measuring microsecond lifetimes should be kHz, and for nanosecond lifetimes the MHz frequency should be used.

The basic principles of a FD FLIM method and our FD FLIM system are illustrated in **Figure 2**. The ISS ALBA system used in this study uses the digital FD technique marketed as FastFLIM (see INTRODUCTION), which uses a pulsed laser as the excitation source and simultaneously measures phase delays and modulation ratios at multiple frequencies. The ISS ALBA FastFLIM system is coupled to an Olympus IX71 microscope equipped with an Olympus ×60/1.2 NA water-immersion objective lens. A 5-mW, 440-nm pulsed diode laser with a pulse width of 8 ns is modulated by the FastFLIM module of the ALBA system at the fundamental frequency of 20 MHz with up to six sinusoidal harmonics. The modulated laser is coupled to the ALBA scanning system that is controlled by ISS VistaVision software. Signals emitted from the specimens were routed by a beam splitter through either a 530/43-nm or 480/40-nm band-pass emission filter, and then detected using

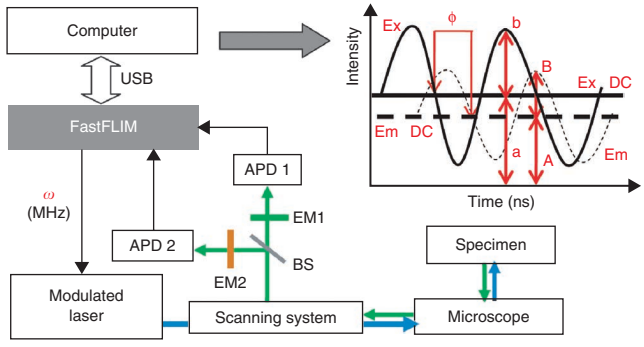

Figure 2 | Frequency-domain (FD) FLIM setup. FD FLIM uses a modulated light source to excite the specimen. The basic principle of the FD FLIM method is illustrated, showing the phase delay (Φ) and modulation ratio (m = (B / A) / (b / a)) of the emission (Em, dashed sinusoidal curve) relative to the excitation (Ex, solid sinusoidal curve), which are used to estimate the fluorescence lifetime. For cyan fluorescent proteins, a 440-nm pulsed-diode laser is directly modulated by the ISS FastFLIM module at the fundamental frequency of 20 MHz with several sinusoidal harmonics. The modulated laser is coupled to the ISS scanning system attached to an Olympus IX71 microscope to scan specimens. Photons emitted from the specimen travel through the scanning system (descanned detection) and are then routed by a beam splitter (BS) through emission (EM) filters to two identical avalanche photodiodes (APD) detectors. The phase delays and modulation ratios of the emission relative to the excitation are measured at up to seven modulation frequencies (ω = 20–140 MHz) for each *XY* raster scanning location, and are also available in *Z* by changing focus. The excitation profile is obtained through a calibration procedure in which a reference fluorophore of known lifetime is used.

two identical APDs. The phase delays and modulation ratios of the emission relative to the excitation were measured at five modulation frequencies (20, 40, 60, 80, 100 MHz) for each pixel of an image. The excitation profile is obtained at the beginning of an experiment using calibration with a standard fluorophore of known lifetime (in our case, Coumarin 6 in ethanol). The measured phase delays and modulation ratios are analyzed by the VistaVision software to extract the lifetime information. The VistaVision software provides both the fitting and phasor plot approaches for data analysis; allows users to specify the number of exponential components for fitting; calculates the standard weighted least squares (χ^2) as a quantitative measurement of the fitting significance; and plots the fitted curve versus the measured data as well as the corresponding residuals for visually assessing the fit. We carried out all the FD FLIM measurements at 22 ± 1 °C in a dark room, using a commercial chambered cover glass to hold our specimens.

PROCEDURE

Cell transfection ● TIMING ~20 h

1| Transfect cells using option A (TCSPC FLIM measurements) or B (FD FLIM measurements). In the examples described here for both methods, the individual plasmid vectors (C5A, C5V, Cerulean-bZip, Venus-bZip, see REAGENT SETUP) and the vector combination (Cerulean-bZip + Venus-bZip in the ratio of 1 to 4) were used for transfecting GHFT1 cells on either cover slips (option A) or cover glass chambers (option B). In addition, untransfected cells are used for checking autofluorescence detected from the cells under the same conditions used for FLIM imaging (see Step 4).

(A) Transfection by FuGENE 6

(i) Prepare the DNA + FuGENE mixtures for transfection. For each DNA + FuGENE mixture, prepare a polystyrene tube with adding 91 µl of serum-free cell culture medium. Thereafter, add FuGENE 6 followed by DNA directly into liquid and tap gently to mix. In our case, we use a FuGENE 6-to-DNA ratio of 8:1 and a total DNA amount of 1 µg.

(ii) Incubate the transfection mixtures for 30–45 min at room temperature.

(iii) Place clean cover slips into a clean six-well dish. Add 1 ml of cell culture medium + NBCS to each cover slip.

(iv) Aspirate medium from the cell culture plate. Add PBS to clean off excess medium. Aspirate PBS.

(v) Add 1 ml of trypsin-EDTA (0.05% (wt/vol) in 0.53 mM EDTA) into the cell culture plate and swirl the plate. Once all of the cells have released from the plate, add the cell culture medium + NBCS into the cell culture plate and swirl.

(vi) Ensure that the cells are evenly distributed by pipetting them in the cell culture plate several times, and then add 1 ml of cells into each well of the six-well dish.

(vii) Add the corresponding DNA + FuGENE 6 mixture to each well slowly while swirling the dish to evenly spread DNA.

(viii) Place cultures in an incubator (37 °C and 5% CO_2) for 18 h before imaging.

(B) Transfection by electroporation

(i) The plasmid vectors encoding the fusion proteins are placed in sterile electroporation cuvettes. The amount of DNA per cuvette typically ranges from 5 to 30 µg, and optimal concentrations must be determined by experimentation; empty plasmid DNA is used to maintain the total amount of DNA constant for any given experiment. Both 0.2- or 0.4-cm gap cuvettes are available, and electroporation conditions must be optimized for each cell line.

(ii) Rinse the cell monolayers in the cell culture flasks with PBS, and then treat the cells with trypsin (0.05% (wt/vol) in 0.53 mM EDTA) for a few seconds. Remove the trypsin solution.

(iii) When cells begin to release from the surface of the flask, recover the cells in cell culture medium containing NCBS. Wash the cells twice by centrifugation in Dulbecco's calcium- and magnesium-free PBS.

(iv) Resuspend the cells to a final concentration of ~1 × 10^7 cells per ml in Dulbecco's calcium- and magnesium-free PBS. Add 400 µl of the cell suspension to each 0.2-cm gap electroporation cuvette containing the DNA.

(v) Gently mix the contents of the cuvette and then pulse the cells at the desired voltage and capacitance. For a 400 µl suspension of cells in 0.2-cm gap cuvettes, we use a 200-V pulse at a total capacitance of 1,200 µF. The typical pulse durations obtained under these conditions are 9–10 ms.

(vi) Immediately recover the cells from the cuvette and dilute in phenol red–free cell-culture medium containing NBCS.

(vii) Inoculate the cells dropwise onto a sterile 22-mm cover glass in 35-mm culture dishes, or, alternatively, a 20-mm chambered cover glass (we used this option). Allow cells to attach to the cover glass for ~20 m at room temperature.

(viii) Gently flood the culture dish with medium and place in an incubator (37 °C and 5% CO_2) for 18 h prior to imaging.

Turn on the FLIM system ● TIMING ~0.5 h

2| Turn on the system according to the manufacturer's instructions. Activate the laser line to be used and select the optical configuration from the system software, e.g., the dichroic mirror, the beam splitter, the emission filters and so on. We performed TCSPC FLIM measurements with the multiphoton laser tuned to 820 nm and one detecting channel (480/40 nm). We carried out FD FLIM measurements with a pulsed-diode 440-nm laser and two detecting channels (the donor channel - 480/40 nm and the acceptor channel - 540/43 nm) (see EQUIPMENT SETUP).

▲ **CRITICAL STEP** Leave the laser on (i.e., warm up the laser) for ~30 min before imaging.

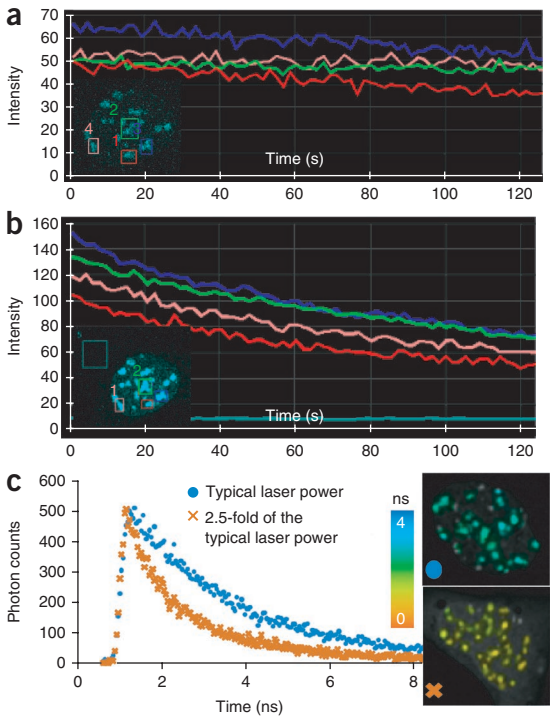

Figure 3 | Photobleaching affects the accuracy of FLIM measurements. Live cells that only express the donor (here, Cerulean-bZip) are used to establish a suitable excitation power level for the TCSPC FLIM-FRET measurements. The amount of photobleaching can be evaluated by monitoring the intensity changes in selected cell regions over time. (**a**) Shown is a typical photobleaching level at the excitation power level used in the TCSPC FLIM-FRET study (~1.2 mW at the specimen plane). (**b**) The increased photobleaching when 250% (2.5-fold) of the excitation power level (~ 3 mW at the specimen plane) is used. (**c**) The effect of the increased photobleaching on the FLIM measurements is shown, demonstrating that the decay profile for Cerulean-bZip is markedly shifted by photobleaching. The mean lifetime obtained from the FLIM data acquired at the high laser power level (~1.3 ns) is much shorter than the normal value (~2.75 ns).

Establish the excitation power ● TIMING ~0.5 h

3| Evaluate the observed photobleaching. At a particular excitation power level, take time-lapse (2–3 min) images of representative donor-alone cells (e.g., in our case, cells that only express Cerulean-bZip) and monitor the intensity changes in selected regions of interest (ROI) in the cells over time (see **Fig. 3**).

▲ **CRITICAL STEP** It is important to establish a suitable excitation power level that produces optimal signals but that does not result in marked photobleaching, as this will affect the accuracy of fluorescence lifetime results (see **Fig. 3** and ref. 79).

▲ **CRITICAL STEP** Photobleaching can be also indicated during FLIM data acquisition, when the rate of photon counts decreases continuously. This rate is usually given by the constant fraction discriminator level of a TCSPC FLIM system, and it is also directly shown by the software in our FD FLIM system. One should avoid using an excitation power level that yields more than ~20% intensity decrease over the timeframe of the experiment. In our TCSPC FLIM measurements, the average excitation power level of the multiphoton laser (tuned to 820 nm) was measured to be ~1.2 mW at the specimen plane. In our FD FLIM measurements, the average excitation power level of the pulsed diode 440 nm laser was measured to be 0.07 mW at the specimen plane.

? TROUBLESHOOTING

Check for autofluorescence ● TIMING ~0.5 h

4| Measure the autofluorescence background from untransfected cells at the excitation wavelength to be used (in our case, 820 nm in TCSPC FLIM and 440 nm in FD FLIM), and at the suitable excitation power level established in Step 3. We detected no noticeable autofluorescence signals in both our TCSPC and FD FLIM measurements.

▲ **CRITICAL STEP** Autofluorescence only needs to be checked the first time a specific experiment is performed; Step 4 does not need to be repeated in subsequent experiments.

? TROUBLESHOOTING

Check for back bleedthrough in a FRET study ● TIMING ~0.5 h

5| Excite cells transfected with only the acceptor fluorophores (Venus-bZip, in our case) at the donor fluorophores excitation wavelength (820 nm in TCSPC FLIM and 440 nm in FD FLIM). Use the excitation power levels established in Step 3 to determine whether there are any bleedthrough signals to the donor channel (480/40 nm in our case). No noticeable back bleedthrough signals were observed for both our TCSPC and FD FLIM measurements.

▲ **CRITICAL STEP** Bleedthrough only needs to be checked the first time a specific experiment is performed; Step 5 does not need to be repeated in subsequent experiments.

? TROUBLESHOOTING

Calibrate the FLIM system ● TIMING ~1 h

6| Calibrate the TCSPC FLIM system as described in option A. Option B should be used to calibrate the FD FLIM system.

(A) Calibrating the TCSPC FLIM system

(i) Measure the IRF of the TCSPC FLIM system equipped with a multiphoton laser: tune the multiphoton laser to an appropriate excitation wavelength (940 nm, in our case) and detect the emission signal at half of the excitation wavelength using the corresponding emission filter (480/40 nm, in our case); scan the urea crystal slide with the same

optics and TCSPC settings used for imaging the biological specimens to record the SHG signals (we used the regular FLIM data acquisition mode of the BH SPCM software, but the 'Single' mode in the SPCM software is also suitable). Save the acquired IRF data.

▲ CRITICAL STEP As the SHG signals are usually very strong, a low excitation power needs to be used to achieve a reasonable photon count rate and avoid the pile-up effect (see Chapter 4 in ref. 1).

? TROUBLESHOOTING

(ii) Measure the fluorescence lifetime standard: add the reference fluorophore solution (in our case Coumarin 6 in Ethanol) to the chamber and focus at the brightest plane, which is the surface between the cover glass and the solution; thereafter, move the focus slightly into the solution to avoid light scattering that occurs at the surface; scan the current field to acquire a TCSPC FLIM data set. Save the acquired data set. Acquire a couple more data sets (three, in our case) in different fields of the solution.

? TROUBLESHOOTING

(iii) Analyze the data acquired from the fluorescence lifetime standard. Data analysis will vary depending on the software used. The basic procedures for analyzing our TCSPC FLIM data using the BH SPCImage software and the measured IRF are described in **Box 1**. The exponential fitting model is chosen according to the reference lifetime standard. We used the monoexponential model to analyze the Coumarin 6 data with the measured IRF obtained as explained in Step 6A(i) (see **Fig. 4**). We also suggest processing the lifetime-standard data with the estimated IRF. In the SPCImage software, the estimated IRF is generated by clicking on 'System Response' under the 'Calculate' menu. In our case, the lifetime of Coumarin 6 obtained with the measured IRF (~2.58 ns) is slightly closer to the reference value (2.5 ns) than that obtained with the estimated IRF (~2.65 ns).

? TROUBLESHOOTING

(B) Calibrating the FD FLIM system

(i) Add the lifetime-standard solution (Coumarin 6 in ethanol, in our case) into a glass chamber. Focus at a plane slightly above the surface between the glass and the solution. Input the lifetime value of the standard (2.5 ns, in our case) into the software (in our case, through the calibration window of the ISS VistaVision software) and then run the calibration for 10 s.

(ii) In the software data acquisition mode, scan the current field of the standard solution to acquire the data until the maximum number of counts per pixel in the donor channel (480/40 nm) reaches more than 100. Save the acquired data set (an '.ifli' file, in our case).

? TROUBLESHOOTING

(iii) Display the Coumarin 6 data acquired in the 480/40-nm channel in the phasor plot. In the ISS VistaVision software, we typically apply a smooth function with the 'Smooth' value of 2, which applies a Gaussian filter to average noisy pixels in the phasor plot. For the fluorescence lifetime standard that is expected to have a monoexponential decay (e.g., Coumarin 6 in ethanol), the center of the distribution of the measured data points should fall on the semicircle of the phasor plot (see **Fig. 5**). Draw a circle covering the points displayed on the phasor plot to measure the mean phase lifetime τ_Φ (see equation (4)) and the mean modulation lifetime τ_m (see equation (5)). The equal phase lifetime and modulation lifetime will provide additional proof that the decay is monoexponential. Run a single exponential fitting on a selected ROI of the image to verify that the lifetime value obtained from the fitting is close to the reference lifetime value.

? TROUBLESHOOTING

(iv) Repeat Steps 7B(ii) and 7B(iii) to acquire more data sets (two, in our case) in different fields of the Coumarin 6 solution.

(v) Add another standard solution (HPTS in phosphate buffer pH 7.5 in our case) into a different glass chamber. Focus at a plane slightly above the surface between the glass and the solution. Repeat the procedures described in Step 7B(ii–iv) to acquire a few data sets (three, in our case) on different fields of the solution. Verify the measured lifetimes with the reference lifetime value. Here, the center of the distribution of the HPTS data points falls exactly on the semicircle of the phasor plot (see **Fig. 5**), indicating a monoexponential decay, as expected; both the phase (5.31 ns) and modulation (5.26 ns) lifetimes are very close to the reference lifetime value (5.3 ns).

Measure FRET of the FRET standard construct ● TIMING 1.5–2 h

7| Measure FRET of the FRET standard construct using the TCSPC FLIM system (option A) or the FD FLIM systems (option B).

(A) Measuring the FRET standard construct using the TCSPC FLIM System

(i) Place the cover slip with cells expressing the donor fluorophore of the FRET standard (C5A in our case) into the chamber. Using the optimal excitation power level established in Step 3, acquire FLIM data sets from a number of cells (ten, in our case). About 1,000–2,000 counts per pixel should be accumulated. The time for data acquisition varies depending on the fluorophore expression level and the sensitivity of the lifetime detector. It took us ~90–180 s to acquire one data set on our TCSPC FLIM system.

BOX 1 | ANALYZING OUR TCSPC FLIM DATA USING BH SPCIMAGE SOFTWARE AND THE MEASURED IRF

1. *Upload the measured IRF data set, generate the IRF and save the IRF into the SPCImage software:* Select 'Import…' under the 'File' menu to load an acquired IRF data set (an '.sdt' file). Click the 'Curve to IRF' symbol to generate the IRF from the data[70]. Click 'Store' under the 'Conditions' menu to save the current fit conditions including the IRF in the software. Close the 'IRF' data set by clicking 'Close' under the 'File' Menu. However, the software must be kept open.
2. *Load the BH FLIM data set (an '.sdt' file) to be processed into the SPCImage software*: Use 'Import…' in the 'File' menu to load the data set.
3. *Apply the IRF saved in Step 1 of this Box to fit the loaded data set*: Click 'Load' under the 'Conditions' menu to apply the IRF stored in the software.
4. *Specify the fitting model and parameters:*
Lifetime constraints: The SPCImage software allows users to set the lifetime constraints, which are used to define a limited space (e.g., 0.1 to 5 ns) to search the lifetime values best fitted to the measured data, rather than using the entire space from zero to infinity. Click 'Model' under the 'Options' menu to specify the minimum and maximum lifetime values under 'Parameter Constraints', based on the expectation of the lifetime values to be resolved. Specifying the proper constraints based on prior knowledge of the expected lifetime values can help the fitting algorithm achieve a faster and more accurate convergence on correct results. However, one should always first try fitting with the default constraints given by the software. In our case, the minimum and maximum lifetime constraints were set to be 0.1 and 5 ns, respectively, as this range (0.1–5 ns) completely covers the expected Coumarin 6 (~2.5 ns) and Cerulean (1–4 ns) lifetime values. We also fitted our data using the default constraints (0.02–30 ns) given by the software and did not obtain any lifetime value beyond 5 ns.
Fitting range: In the SPCImage software, the measured decay data points at one cursor location and the corresponding fitting curve are shown in the 'Decay Graph' panel with the time (0–10 ns in our case) as the horizontal axis and the number of photon counts as the vertical axis. It is usually better to fit the data points within a certain range of time channels of a decay trace than those of the whole decay trace. The starting and ending time channels for the fitting range are defined by 'T1' and 'T2', respectively, shown above the 'Decay Graph' panel. In our case, 'T1' is set as the time channel right after the rising point of a decay trace (~0.8 ns) and the default 'T2' given by the software (~8.5 ns) is used.
Exponential model: The SPCImage software allows fitting with up to three components. Under the 'Multiexponential Decay' panel, specify the number of 'Components' (lifetime components described by equation (1)). Before determining the exponential model, one should always compare the single versus the double versus even the triple exponential fittings at number of representative cursor locations. The weighted least squares value (shown as 'χr_2' in the software) can be a good indicator for the evaluation of the fitting significance. It is important to note that the comparison is reproducible over many pixels. It should be noted that a robust fitting usually requires a certain number of photon counts, which would depend on the complexity of the fitting model (discussed below in *Binning*). For the other parameters in the 'Multiexponential Decay' panel such as 'Shift', 'Scatter' and 'Offset', we typically have them optimized by the fitting algorithm with the 'Fix' box unchecked. To evaluate how the value of a parameter affects fitting, one can check the 'Fix' box for the parameter and manually change the parameter value while leaving the other parameters to be optimized by the software.
Binning: The binning option is selected if there are insufficient photon counts at each pixel. It is usually helpful to group neighbored pixels together into one decay trace to achieve enough photon counts for a robust fitting, although the spatial resolution will be sacrificed. This is often termed as binning. In the SPCImage software, the binning is applied by giving a proper 'Bin' value above the 'Decay Graph' panel. As a rule of thumb given in the SPCImage software manual, the peak photon count level along a decay trace (after binning) should at least reach 100, 1,000 and 10,000 for a single, double and triple exponential fitting, respectively.
Threshold: The SPCImage software allows users to set a threshold (labeled as 'Thld' above the 'Decay Graph' panel) for the peak photon count level of a decay trace, based on which of the pixels not having enough photon counts (after binning) will not be fitted. For some biological applications, setting a proper threshold can help segment the ROIs out of the whole image. *Note:* All above fitting options (once defined) can be saved by clicking 'Store' under the 'Conditions' menu and then be reapplied to process another data set by clicking 'Load' under the 'Conditions' menu.
5. *Run fitting on the whole image or a selected ROI on the image*: In the SPCImage software, fitting will be only be applied to the pixels within the square region defined by the two cursors shown on the lower left and upper right corners of the image. By default, the region covers the whole image, but this region can be changed by moving the two cursors. Clicking 'Decay Matrix' under the 'Calculate' menu will run fitting on the defined region.
6. *Plot the lifetime distributions, record the statistics and save the analyzed data*: After fitting, the SPCImage software by default will show a color-coded lifetime image. The color indicates the lifetime value, e.g., red (shorter lifetime) to green to blue (longer lifetime). The lifetime distribution for each component can be plotted given the 'Coding of Value' by clicking 'Color' under the 'Options' menu. For example, when a biexponential fitting model ('Components' = 2) is applied, selecting 't1' or 't2' as the 'Coding of Value' will display the distribution for the shorter or the longer lifetime components, respectively, and choosing 'tm' will show the distribution of the average (or apparent) lifetime (τ_a defined by equation (2)). At selected ROIs, record the mean values for the weighted least squares (labeled as 'Chi', the apparent lifetime ('tm'), each lifetime component ('t1', 't2', 't3') and its associated pre-exponential factor ('a1', 'a2', 'a3'). Finally, remember to save the analyzed data (an '.img' file, in our case).

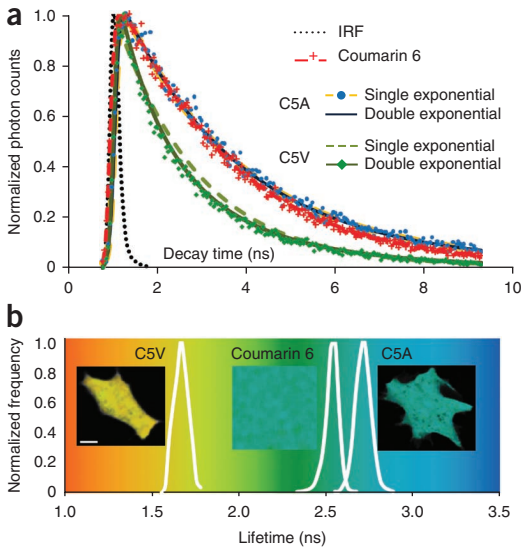

Figure 4 | TCSPC FLIM data representation of the FRET standard. (**a**) The representative Coumarin 6, C5A (donor-alone control) and C5V (FRET standard) raw decay data and corresponding fitting curves are shown. Fittings were carried out using the measured instrument response function (IRF) with a full width at half maximum of ~300 ps. The fluorescent lifetime decay kinetics for Cerulean in the C5A and C5V constructs was determined through the comparisons of fitting the decay data into both single- and double-exponential decay models. There was little difference observed between the single- and double-exponential fits of the C5A decay data, confirmed by the calculated χ^2s—1.08 (single) versus 1.07 (double). However, the C5V FRET standard was better represented by the double-exponential fit (χ^2 = 1.07) compared with the single-exponential fit (χ^2 = 2.38). The results clearly show the quenched state of Cerulean (the donor) in the presence of Venus (the acceptor) resulting from FRET. (**b**) The lifetime distributions in representative Coumarin 6, C5A or C5V lifetime (overlaid with intensity) images are shown (the apparent lifetime for C5V, see equation (2)). Scale bar, 10 μm.

(ii) Repeat Step 7A(i) with the cover slip of cells expressing both the donor and the acceptor of the FRET standard (C5V, in our case).

(B) Measuring the FRET standard construct using the FD FLIM system

(i) Using the glass chamber with the cells that only express the donor of the FRET standard (C5A, in our case) and the optimal excitation power level established in Step 3, acquire the FLIM data sets from a number of cells (ten, in our case). The maximum number of counts per pixel in the donor channel (480/40 nm) should reach more than 100. The time for data acquisition varies according to the fluorophore expression level and the sensitivity of the lifetime detector. It took us ~30–60 s to acquire one data set.

(ii) Repeat Step 7B(i) with the glass chamber of cells expressing both the donor and the acceptor of the FRET standard (C5V, in our case). The maximum number of counts per pixel in the donor channel (480/40 nm) should be more than 200. **? TROUBLESHOOTING**

Measure FRET of the biological system ● TIMING 1.5–2 h

8| Measure FRET of the biological system using the TCSPC FLIM system (option A) or the FD FLIM systems (option B).

(A) Measuring FRET of the biological system using the TCSPC FLIM system

(i) Place the cover slip with cells that only express the donor of the biological system (Cerulean-bZip in our case) into the chamber. It should be noted that temperature and CO_2 control may be required in some biological systems under investigation. Use the optimal excitation power level established in Step 3 to acquire the FLIM data sets for a number of cells (ten, in our case). About 1,000–2,000 counts per pixel should be accumulated. In our case, it took ~90–180 s to acquire one data set.

(ii) Repeat Step 8A(i) with the cover slip of cells coexpressing the donor (Cerulean-bZip) and the acceptor (Venus-bZip, in our case) of the biological system. It is important to recognize that, unlike the FRET standard protein (C5V) in which the donor and the acceptor are directly linked and always at a 1:1 ratio, the Cerulean-bZip and Venus-bZip proteins are independently expressed. This means that every transfected cell will have a different donor-to-acceptor ratio.

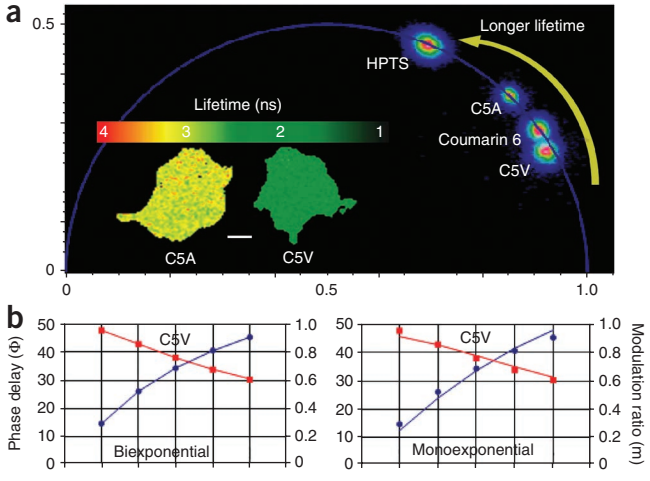

Figure 5 | FD FLIM data representation of the FRET standard. (**a**) The representative HPTS, Coumarin 6, C5A (donor-alone control) and C5V (FRET standard) data measured at the fundamental modulation frequency (20 MHz) are displayed in the phasor plot. Both HPTS and Coumarin 6 are expected to have a single lifetime component, and this is clearly shown by the phasor plot, in which the lifetime distributions are centered on the universal semicircle of the phasor plot. This is also observed for the lifetime distribution for the cell expressing the C5A fusion protein. (**b**) However, the lifetime distribution for the cell expressing the C5V fusion protein falls inside the semicircle, and is better fitted with a biexponential model than a monoexponential model, as shown. As HPTS (~5.3 ns) has a much longer lifetime than Coumarin 6 (~2.5 ns), the two populations in the phasor plot are well separated. The phasor plot clearly demonstrates the quenching of the donor (Cerulean) in the C5V protein compared with the unquenched donor in C5A. Scale bar, 10 μm.

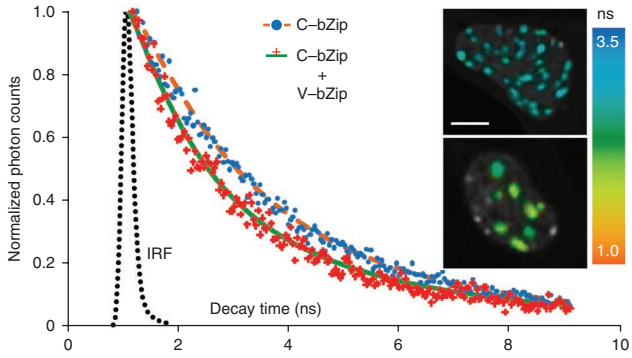

Figure 6 | Localization of dimerized C/EBPα-bZip in living cell nucleus using TCSPC FLIM-FRET microscopy. C/EBPα-bZip was tagged with either Cerulean (C) or Venus (V). The fluorescent lifetime decay kinetics for the C–bZip (FRET donor) in the absence and the presence of V–bZip (FRET acceptor) was determined by fitting the measured decay data into a single or double-exponential decay model, respectively, with the measured instrument response function (IRF). Use of a threshold allowed fitting to the pixels in regions of centromeric heterochromatin of the cell nucleus. The comparison between the representative measured decay data points, the fitting curves and the lifetime (overlaid with intensity) images of the two cases clearly shows that the C in cells expressing both C–bZip and V–bZip decayed faster (or has a shorter lifetime) than that in cells expressing C–bZip alone, indicating that the C attached to bZip was quenched by the V attached to bZip because of FRET. Scale bar, 10 μm.

(B) Measuring FRET of the biological system using the FD FLIM system

(i) Place the glass chamber with the cells that only express the donor of the biological system (Cerulean-bZip, in our case). Use the optimal excitation power level established in Step 3 to acquire the FLIM data sets from number of cells (ten, in our case). The maximum number of counts per pixel in the donor channel (480/40 nm) should reach more than 100. In our case, it took ~30–60 s to acquire one data set.

(ii) Repeat Step 8B(i) with the glass chamber of cells expressing both the donor (Cerulean-bZip) and the acceptor (Venus-bZip, in our case) of the biological system. Our FD FLIM system is equipped with two lifetime detectors, and thus allows us to simultaneously acquire the signals in both the donor (480/40 nm) and the acceptor (540/43 nm) channels. This is especially helpful for a biological system in which the donor and the acceptor proteins are independently expressed, e.g., the bZip biological model described here (see Step 9B(ii)). The maximum number of counts per pixel in the donor channel (480/40 nm) should be more than 200.

? TROUBLESHOOTING

Analyze the FLIM-FRET Data ● TIMING 2–3 h

9| Analyze the TCSPC FLIM-FRET data as described in option A. Option B should be used to analyze the FD FLIM-FRET data.

(A) Analyze the TCSPC FLIM-FRET data

(i) Follow the steps described in **Box 1** to analyze the C5A data sets using the measured IRF obtained in Step 6A(i). In our case, the monoexponential model was applied to fit the C5A data, as the fitting was not obviously improved by adding one more exponent (**Box 1** and **Fig. 4**). A threshold of 20 was used to separate the pixels in cells (to be fitted) from the background pixels (**Box 1**). Summarize the statistics for all analyzed C5A data sets. It is important that the results be reproducible across different cells.

(ii) Follow the steps described in **Box 1** to analyze the C5V data sets. In our case, the biexponential model was used to fit the C5V data, because of a significant improvement of the fitting compared with using one exponential component (see **Fig. 4**). However, no improvement was observed for the fitting with three exponents (data not shown). Summarize the statistics for all analyzed C5V data sets.

(iii) Use the mean of the Cerulean lifetimes determined from all C5A cells as τ_D and the mean of the apparent lifetimes of Cerulean in a ROI of a C5V cell as the τ_{DA} to calculate energy transfer efficiency (E) for the ROI of the C5V cell based on equation (3). Summarize the statistics for all selected ROIs.

(iv) Follow the steps described in **Box 1** and the logics described in Step 9A(i–iii) to analyze the data sets acquired from the cells that only express the donor (Cerulean-bZip in our case), and the cells expressing both the donor (Cerulean-bZip) and the acceptor (Venus-bZip in our case). Here, the Cerulean-bZip data were well fitted with a monoexponential model and the 'Cerulean-bZip + Venus-bZip' data were fitted better with a biexponential model (see **Fig. 6**). In many cases, lifetimes are only interesting in specific cellular compartments. It is critical to measure the lifetimes at the same cellular compartments for both donor-alone control cells and cells containing both donor and acceptor. Here, we applied a threshold to the expression level of a cell to ensure fitting only of the pixels in regions of centromeric heterochromatin in the cell nuclei (see **Fig. 6** and ANITCIPATED RESULTS).

(B) Analyze the FD FLIM-FRET data

(i) Follow the procedures described in Step 6B(iii) to analyze the C5A and C5V data sets. Here, a 'Threshold' value in the ISS VistaVision software was used to exclude the background pixels. We fitted the C5A data with a monoexponential model to estimate its lifetime, because the distribution of the data points centers on the semicircle of the phasor plot (**Fig. 5**). However, most of the C5V data points fall inside the semicircle of the phasor plot (**Fig. 5**), indicating a

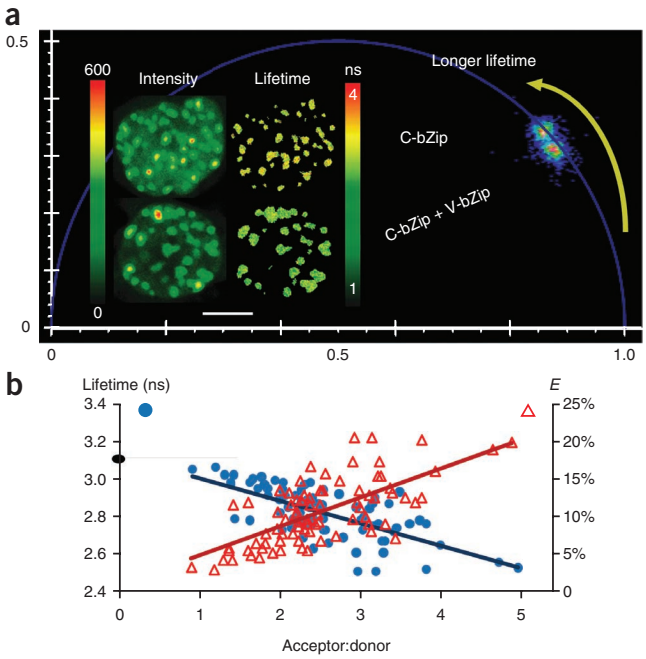

Figure 7 | Investigation of the dimerization of C/EBPα-bZip in living cell nucleus using FD FLIM-FRET microscopy. bZip was tagged with either Cerulean (C) or Venus (V). (**a**) The intensity and lifetime images of representative cells, which only express C–bZip (donor-alone control) and that co-express C–bZip (FRET donor) and V–bZip (FRET acceptor), are compared. The FD FLIM data acquired at the fundamental modulation frequency (20 MHz) is displayed on the phasor plot. The comparison demonstrates a shorter lifetime of Cerulean in the cell that expresses both C–bZip and V–bZip. The lifetimes of C–bZip in the absence and the presence of V–bZip were estimated by single- and double-exponential fittings, respectively. (**b**) The average donor lifetime, obtained from ten cells that expressed only C–bZip, was 3.15 ns (indicated by the black dot). The apparent lifetimes for 80 regions of interest (ROIs) identified in ten cells coexpressing C–bZip and V–bZip were then determined, and the range was from 2.5 to 3.05 ns, resulting in a variety of energy transfer efficiencies (*E*) calculated on the basis of equation (3). To investigate how the quenched C–bZip lifetimes were influenced by the acceptor-to-donor ratio, we roughly determined the ratio using the intensities obtained in the acceptor and donor channels for each ROI. With all 80 ROIs, the lifetime (blue dots with a dark blue trend line: $R = 0.35$) or *E* (red triangles with a dark red trend line: $R = 0.19$) shows a negative or positive dependency on the acceptor-to-donor ratio, respectively (scale bar, 10 μm).

multiexponential case. The C5V data were well fitted with a biexponential model (see **Fig. 5**), resulting in the average apparent lifetime of 1.89 ns (τ_{DA}) and the *E* of 39.8% calculated based on equation (3) using the mean C5A lifetime of 3.14 ns as τ_D.

(ii) Follow Steps 6B(iii) and 9B(i) to analyze the Cerulean-bZip (donor-alone control) and 'Cerulean-bZip + Venus-bZip' data sets. Here, number of ROIs were selected in regions of centromeric heterochromatin in the cell nuclei. The data of each ROI in the donor-alone cells were well fitted by a monoexponential model to estimate the average unquenched Cerulean lifetime (τ_D) for determining *E*. For the data acquired from the cells coexpressing the Cerulean-bZip and Venus-bZip constructs, the double-exponential fitting yielded the best results, and for each selected ROI, we measured the apparent lifetime as the quenched Cerulean lifetime (τ_{DA}) for *E* calculation, and also the ratio between the intensities obtained in the acceptor channel versus the donor channel. By using all the ROIs selected from many cells coexpressing donor and acceptor, we investigated how the apparent lifetimes and *E*s are dependent on the estimated acceptor-to-donor ratios (see **Fig. 7** and ANTICIPATED RESULTS).

? TROUBLESHOOTING

Troubleshooting advice can be found in **Table 1**.

TABLE 1 | Troubleshooting table.

Step	Problem	Possible reason	Solution
3	The photon counts rate fluctuates during FLIM data acquisition	The excitation light source is unstable, which can be caused by variations in room temperature or the misalignment of the excitation source	Check the laser alignment; check the cable connection; call system service
	Photobleaching is observed	The power of the excitation light is too high	Reduce the average power of the excitation light; add antiphotobleaching agent if it does not interfere with the selected biological investigation (Step 1)
		Cells do not adhere to the cover slip properly, or they are not healthy	Repeat cell preparation (Step 1)

(continued)

TABLE 1 | Troubleshooting table (continued).

Step	Problem	Possible reason	Solution
4	Considerable autofluorescence is detected	Some molecules in the specimen have absorption properties at the excitation wavelength	The autofluorescence may be reduced by selecting an appropriate excitation wavelength if a tunable laser is used. Otherwise, the lifetime of the autofluorescence must be measured from the untransfected (or unlabeled) specimens and this lifetime information needs to be considered in further FLIM data analysis
5	Substantial bleedthrough signal from the acceptor to the donor channel is observed	The acceptor fluorophore has a considerable absorption rate at the donor excitation wavelength	Use a different acceptor fluorophore, as the bleedthrough signals from the acceptor to the donor channel will markedly complicate FLIM-FRET data analysis. When a tunable laser is used, try to select an appropriate donor excitation wavelength to avoid the bleedthrough
6A(i)	There is more than one peak in the measured IRF of the FLIM system	This probably caused by the multiple reflections detected by the lifetime detector, e.g., the condenser of an inverted microscope can be an unwanted reflection source	Cover the specimen chamber with a black box to avoid the reflection from the condenser of an inverted microscope. As lifetime detectors are highly sensitive, any ambient light should be avoided during FLIM data acquisition
6A(ii) and B(ii)	The achieved photon counts level is lower than that usually obtained for the same fluorophore solution during the same acquisition time	Misalignment of the laser, especially when a manually tunable multiphoton laser is used	Check the laser alignment or call system service
		Mismatching of the photon arrival to the detector and the reference pulse in a TCSPC system	Check the synchronization of the excitation pulse with the TCSPC system and the threshold level setup in the constant fraction discriminator (CFD); call system service
		Shift of the confocal pinhole position when a confocal pinhole is used	Adjust the pinhole position to reach the expected photon counts level
6A(iii) and B(iii)	The measured lifetime of the fluorescence lifetime standard is different than the literature value	The lifetime standard chemical may be out of date	Repeat the measurement with the freshly prepared lifetime standard
		The literature value may be wrong	Measure some other fluorescence lifetime standards
		The lifetime standard is not prepared exactly according to the literature	Prepare the lifetime standard exactly as instructed in the literature
7	The fluorescent proteins are overly expressed or the fluorescent protein expression level is very low	The transfection agent (FuGENE, Lipofectamine, etc.) or DNA plasmid concentration or their ratio is not optimized	Follow the transfection agent manufacturer's recommendations to vary the ratio of DNA: transfection agent or concentrations of DNA and/or transfection agent
8	Inconsistent results are obtained	Inconsistency in the biological samples; changes introduced to the biological system (such as pH, temperature) may perturb the lifetimes of the fluorophores to be measured	Carefully check the procedures for preparing the biological samples. Make sure to use the same biological assay to prepare specimens for subsequent experiments

(continued)

TABLE 1 | Troubleshooting table (continued).

Step	Problem	Possible reason	Solution
		Inconsistency in the FLIM system; FLIM system performance can be influenced by the changes of its environment (e.g., building vibration, temperature variation)	A FLIM system should be located away from the magnetic field or any instruments that operate on the basis of magnetic fields (e.g., NMR); magnetic fields will damage the lifetime detector. Magnetic field interference can be avoided by putting a wire mesh around the whole system or the detector
			The FLIM system should be ideally placed on an antivibration table on a ground floor or basement. High-level vibration isolation is required if the system is installed above the ground floor of the building
			The room temperature should not vary by more than ±2 °C
			System calibration should be repeated every couple of hours to identify whether the FLIM system only remains consistent for a certain period of time

● **TIMING**

Step 1, Cell transfection: ~20 h, including ~18 h of incubation before imaging
Step 2, Turn on the system and select the optical configuration: ~0.5 h
Step 3, Establish the suitable excitation power: ~0.5 h
Step 4, Check for autofluorescence: ~0.5 h, once per experiment (need not be repated for each experiment for a particular assay)
Step 5, Check for back bleedthrough in a FRET study: ~0.5 h, once per experiment (need not be repeated for each experiment for a particular assay)
Step 6, Calibrate the FLIM system: ~1 h
Step 7, Measure the FRET of the FRET standard construct: 1.5–2 h (only needs to be verified once for a particular system configuration)
Step 8, Measure the FRET of the biological system: 1.5–2 h, depending on the number of FLIM data sets to be acquired, the expression level of the biological system and the photon collection efficiency and the configuration of the FLIM system
Step 9, Analyze the FLIM-FRET data: 2–3 h, depending on the number of FLIM data set to be analyzed and the degree of the analysis

ANTICIPATED RESULTS

Photobleaching should be minimized for FLIM data acquisition. In **Figure 3c**, the fluorescence lifetime results obtained with minimal versus substantial photobleaching are compared, showing that significant photobleaching can result in inaccurate fluorescence lifetime results. When fitting is used in FLIM data analysis, a robust fitting routine needs to be established for a particular data processing model and the reproducibility of data is critical (see INTRODUCTION). For example, it is shown in both **Figures 4a** and **5b** that fitting the C5V data on the basis a monoexponential model will yield incorrect results.

In general, standard fluorophores of known lifetimes should be used to calibrate or adjust the FLIM system parameters before imaging any biological specimens. With a standard fluorophore that is expected to have a monoexponential decay, the measured lifetime should be close to the reference lifetime value. A small difference can be caused by different accuracies of the FLIM systems and also by different imaging environments (for example, different ambient temperature). However, the lifetime standard needs to be carefully prepared according to the reference.

Before studying the protein-protein interactions of a biological system in FLIM-FRET, the FRET standard approach should be initially used to evaluate the FLIM system. The C5A and C5V lifetimes measured by different FLIM systems may vary depending on the expressed cellular environment, their folding properties, accuracy of the FLIM system and so on, and thus may result in different energy transfer efficiencies (*E*s). However, the lifetimes of C5A or C5V expressed in a consistent cellular environment should have a Gaussian distribution with a small variance (see **Figs. 4b** and **5a**). For example, in our

TCSPC FLIM measurements, the lifetimes of C5A (from ten cells) have a mean value of 2.75 ns (τ_D) with a standard deviation of 0.08 ns (χ^2 = 1.08 ± 0.07), and the apparent lifetimes of C5V (from ten cells) have a mean value of 1.66 ns (τ_{DA}) with a standard deviation of 0.05 ns (χ^2 = 1.06 ± 0.02), resulting in an average *E* of 39.6% with a standard deviation of 3%. One would expect a monoexponential decay for C5V, as Cerulean and Venus are linked in a rigid way. However, FRET requires not only a close distance between donor and acceptor, but also a favorable orientation between the dipoles of the donor emission and the acceptor absorption, which may not be satisfied for all C5V constructs. Another cause might be that the linking peptide chain is flexible, whereas donor and acceptor fluorophores are not separated by a single distance rather than by multiple proximity. Moreover, occasional incomplete synthesis or protein misfolding cannot be ruled out. To assess the sensitivity of a FLIM system for a FRET study, it is suggested to measure a series of 'FRET standard' constructs, e.g., C5V, C17V, C32V and CTV. For C17V and C32V, Cerulean (C) and Venus (V) are tethered by either a 17- or 32-aa linker[61]. These FRET standard constructs were clearly distinguished in our earlier TCSPC and DFD FLIM-FRET measurements[80,] and also by others[61,73].

The bZip region of C/EBPα binds as an obligate dimer to α-satellite repeat sequences in regions of heterochromatin, which are especially prominent in mouse cells (see **Figs. 6** and **7**). Here, FLIM-FRET was used to measure dimerization of the Cerulean (FRET donor)- and Venus (FRET acceptor)-tagged C/EBPα–bZip domains in the nuclei of mouse pituitary GHFT1 cells. Because the donor- and acceptor-tagged fusion proteins were expressed independently, each cell that was imaged had a slightly different acceptor-to-donor ratio, and this affected *E*. For TCSPC FLIM-FRET, the average unquenched Cerulean lifetime obtained from measuring 10 cells only expressing Cerulean-bZip was 2.75 ns. The quenched Cerulean-B-ZIP lifetimes measured from 10 cells coexpressing Cerulean-bZip and Venus-bZip ranged from 2.0 to 2.6 ns. In FD FLIM-FRET, for each of 80 ROIs selected from ten doubly expressed cells, we estimated the quenched donor lifetime, calculated the *E* and roughly determined the acceptor-to-donor ratio. Plotting the quenched donor lifetimes (or the *E*s) versus the acceptor-to-donor ratios for all 80 ROIs indicates a negative (or positive) dependency of the quenched donor lifetime (or the *E*) on the acceptor-to-donor ratio (see **Fig. 7**), as expected for the C/EBPα dimerization model.

Note: Supplementary information is available via the HTML version of this article.

ACKNOWLEDGMENTS We acknowledge funding from the University of Virginia, National Center for Research Resources NCRR-NIH RR027409 and National Heart, Lung, and Blood Institute (NHLBI) P01HL101871 (A.P.), and National Institutes of Health (NIH) grants 2RO1 DK43701 and 3RO1 DK43701-15S1 (R.N.D.). We also thank K. Christopher (Biology, University of Virginia) and N. Hays (Indiana University School of Medicine) for preparing the samples, S. Vogel (NIH/NIAAA) for providing the FRET standard constructs, and M. Davidson (National High Magnetic Field Laboratory of Florida State University) for providing the mVenus C1 vector. We express sincere thanks to W. Becker (Becker & Hickl) and B. Barbieri (ISS) for their valuable feedback.

AUTHOR CONTRIBUTIONS All authors contributed equally to the paper. A.P. is one of the pioneers in FLIM imaging technology development for biological applications.

COMPETING FINANCIAL INTERESTS The authors declare no competing financial interests.

Published online at http://www.natureprotocols.com/.
Reprints and permissions information is available online at http://www.nature.com/reprints/index.html.

1. Lakowicz, J.R. *Principles of Fluorescence Spectroscopy* (Springer, 2006).
2. Clegg, R.M. Fluorescence lifetime-resolved imaging: what, why, how—a prologue. In *FLIM Microscopy in Biology and Medicine* (eds. Periasamy, A. & Clegg, R.M.) 3–34 (CRC Press, 2009).
3. Phipson, T.L. *Phosphorescence or the Emission of Light by Minerals, Plants and Animals*. (L. Reeve & Co, 1870).
4. Venetta, B.D. Microscope phase fluorometer for determining the fluorescence lifetimes of fluorochromes. *Rev. Sci. Instrum.* **30**, 450–457 (1959).
5. Periasamy, A. & Clegg, R.M. FLIM applications in the biomedical sciences. In *FLIM Microscopy in Biology and Medicine* (eds. Periasamy, A. & Clegg, R.M.) 385–400 (CRC Press, 2009).
6. Agronskaia, A.V., Tertoolen, L. & Gerritsen, H.C. High frame rate fluorescence lifetime imaging. *J. Phys. D.* **36**, 1655–1662 (2003).
7. Appelblom, H. *et al.* Homogeneous TR-FRET high-throughput screening assay for calcium-dependent multimerization of sorcin. *J. Biomol. Screen* **12**, 842–848 (2007).
8. Vishwasrao, H.D., Heikal, A.A., Kasischke, K.A. & Webb, W.W. Conformational dependence of intracellular NADH on metabolic state revealed by associated fluorescence anisotropy. *J. Biol. Chem.* **280**, 25119–25126 (2005).
9. Wang, H.W. *et al.* Differentiation of apoptosis from necrosis by dynamic changes of reduced nicotinamide adenine dinucleotide fluorescence lifetime in live cells. *J. Biomed. Opt.* **13**, 054011 (2008).
10. Konig, K., Schneckenburger, H. & Hibst, R. Time-gated in vivo autofluorescence imaging of dental caries. *Cell. Mol. Biol. (Noisy-le-grand)* **45**, 233–239 (1999).
11. Ehlers, A., Riemann, I., Stark, M. & Konig, K. Multiphoton fluorescence lifetime imaging of human hair. *Microsc. Res. Tech.* **70**, 154–161 (2007).
12. Uchugonova, A. & Konig, K. Two-photon autofluorescence and second-harmonic imaging of adult stem cells. *J. Biomed. Opt.* **13**, 054068 (2008).
13. Berezovska, O. *et al.* Familial Alzheimer's disease presenilin 1 mutations cause alterations in the conformation of presenilin and interactions with amyloid precursor protein. *J. Neurosci.* **25**, 3009–3017 (2005).
14. Eckert, H., Petrášek, Z. & Kemnitz, K. Application of novel low-intensity nonscanning fluorescence lifetime imaging microscopy for monitoring excited state dynamics in individual chloroplasts and living cells of photosynthetic organisms. *Proc. SPIE* **6372**, 637207 (2006).
15. Petrasek, Z., Eckert, H.J. & Kemnitz, K. Wide-field photon counting fluorescence lifetime imaging microscopy: application to photosynthesizing systems. *Photosynth Res.* **102**, 157–168 (2009).
16. Wouters, F.S. & Bastiaens, P.I. Fluorescence lifetime imaging of receptor tyrosine kinase activity in cells. *Curr. Biol.* **9**, 1127–1130 (1999).
17. Chen, Y., Mills, J.D. & Periasamy, A. Protein localization in living cells and tissues using FRET and FLIM. *Differentiation* **71**, 528–541 (2003).
18. Krishnan, R.V., Masuda, A., Centonze, V.E. & Herman, B. Quantitative imaging of protein-protein interactions by multiphoton fluorescence lifetime imaging microscopy using a streak camera. *J. Biomed. Opt.* **8**, 362–367 (2003).
19. Biskup, C., Zimmer, T. & Benndorf, K. FRET between cardiac Na^+ channel subunits measured with a confocal microscope and a streak camera. *Nat. Biotechnol.* **22**, 220–224 (2004).
20. Chen, Y. & Periasamy, A. Characterization of two-photon excitation fluorescence lifetime imaging microscopy for protein localization. *Microsc. Res. Tech.* **63**, 72–80 (2004).
21. Biener, E. *et al.* Quantitative FRET imaging of leptin receptor oligomerization kinetics in single cells. *Biol. Cell.* **97**, 905–919 (2005).
22. Wallrabe, H. & Periasamy, A. Imaging protein molecules using FRET and FLIM microscopy. *Curr. Opin. Biotechnol.* **16**, 19–27 (2005).
23. Periasamy, A. & Day, R.N. *Molecular Imaging: FRET Microscopy and Spectroscopy* (Oxford University Press, 2005).
24. Forde, T.S. & Hanley, Q.S. Spectrally resolved frequency domain analysis of multi-fluorophore systems undergoing energy transfer. *Appl. Spectrosc.* **60**, 1442–1452 (2006).

25. Biskup, C. *et al.* Multi-dimensional fluorescence lifetime and FRET measurements. *Microsc. Res. Tech.* **70**, 442–451 (2007).
26. Periasamy, A. & Clegg, R.M. *FLIM Microscopy in Biology and Medicine* (CRC Press, 2009).
27. Sun, Y., Wallrabe, H., Seo, S.A. & Periasamy, A. FRET microscopy in 2010: The legacy of Theodor Forster on the 100th anniversary of his birth. *Chemphyschem* **12**, 462–474 (2011).
28. Förster, T. Delocalized excitation and excitation transfer. In *In Modern Quantum Chemistry* (ed. Sinanoglu, O.) 93–137 (Academic Press, 1965).
29. Clegg, R.M. Fluorescence resonance energy transfer. In *Fluorescence Imaging Spectroscopy and Microscopy* (eds. Wang, X.F. & Herman, B.) 179–251 (John Wiley & Sons, 1996).
30. Jares-Erijman, E.A. & Jovin, T.M. FRET imaging. *Nat. Biotechnol.* **21**, 1387–1395 (2003).
31. Sekar, R.B. & Periasamy, A. Fluorescence resonance energy transfer (FRET) microscopy imaging of live cell protein localizations. *J. Cell Biol.* **160**, 629–633 (2003).
32. Vogel, S.S., Thaler, C. & Koushik, S.V. Fanciful FRET. *Sci. STKE* **2006**, re2 (2006).
33. Piston, D.W. & Kremers, G.J. Fluorescent protein FRET: the good, the bad and the ugly. *Trends Biochem. Sci.* **32**, 407–414 (2007).
34. Gadella, T.W.J. *FRET and FLIM Techniques* (Elsevier, 2009).
35. Periasamy, A., Elangovan, M., Elliott, E. & Brautigan, D.L. Fluorescence lifetime imaging (FLIM) of green fluorescent fusion proteins in living cells. *Methods Mol. Biol.* **183**, 89–100 (2002).
36. Periasamy, A. *Methods In Cellular Imaging* (Oxford University Press, 2001).
37. Wallrabe, H., Elangovan, M., Burchard, A., Periasamy, A. & Barroso, M. Confocal FRET microscopy to measure clustering of ligand-receptor complexes in endocytic membranes. *Biophys. J.* **85**, 559–571 (2003).
38. Demarco, I.A., Periasamy, A., Booker, C.F. & Day, R.N. Monitoring dynamic protein interactions with photoquenching FRET. *Nat. Methods* **3**, 519–524 (2006).
39. Chen, Y., Mauldin, J.P., Day, R.N. & Periasamy, A. Characterization of spectral FRET imaging microscopy for monitoring nuclear protein interactions. *J. Microsc.* **228**, 139–152 (2007).
40. Li, H., Li, H.F., Felder, R.A., Periasamy, A. & Jose, P.A. Rab4 and Rab11 coordinately regulate the recycling of angiotensin II type I receptor as demonstrated by fluorescence resonance energy transfer microscopy. *J. Biomed. Opt.* **13**, 031206 (2008).
41. Day, R.N., Booker, C.F. & Periasamy, A. Characterization of an improved donor fluorescent protein for Forster resonance energy transfer microscopy. *J. Biomed. Opt.* **13**, 031203 (2008).
42. Periasamy, A., Wallrabe, H., Chen, Y. & Barroso, M. Chapter 22: Quantitation of protein-protein interactions: confocal FRET microscopy. *Methods Cell Biol.* **89**, 569–598 (2008).
43. Sun, Y. *et al.* Characterization of an orange acceptor fluorescent protein for sensitized spectral fluorescence resonance energy transfer microscopy using a white-light laser. *J. Biomed. Opt.* **14**, 054009 (2009).
44. Li, H. *et al.* Actin cytoskeleton-dependent Rab GTPase-regulated angiotensin type I receptor lysosomal degradation studied by fluorescence lifetime imaging microscopy. *J. Biomed. Opt.* **15**, 056003 (2010).
45. Day, R.N., Periasamy, A. & Schaufele, F. Fluorescence resonance energy transfer microscopy of localized protein interactions in the living cell nucleus. *Methods* **25**, 4–18 (2001).
46. Gratton, E., Breusegem, S., Sutin, J., Ruan, Q. & Barry, N. Fluorescence lifetime imaging for the two-photon microscope: time-domain and frequency-domain methods. *J. Biomed. Opt.* **8**, 381–390 (2003).
47. Colyer, R.A., Lee, C. & Gratton, E. A novel fluorescence lifetime imaging system that optimizes photon efficiency. *Microsc. Res. Tech.* **71**, 201–213 (2008).
48. Elangovan, M., Day, R.N. & Periasamy, A. Nanosecond fluorescence resonance energy transfer-fluorescence lifetime imaging microscopy to localize the protein interactions in a single living cell. *J. Microsc.* **205**, 3–14 (2002).
49. Buranachai, C., Kamiyama, D., Chiba, A., Williams, B.D. & Clegg, R.M. Rapid frequency-domain FLIM spinning disk confocal microscope: lifetime resolution, image improvement and wavelet analysis. *J. Fluoresc.* **18**, 929–942 (2008).
50. Gerritsen, H.C., Asselbergs, M.A., Agronskaia, A.V. & Van Sark, W.G. Fluorescence lifetime imaging in scanning microscopes: acquisition speed, photon economy and lifetime resolution. *J. Microsc.* **206**, 218–224 (2002).
51. Grant, D.M. *et al.* High speed optically sectioned fluorescence lifetime imaging permits study of live cell signaling events. *Opt. Express* **15**, 15656–15673 (2007).
52. McGinty, J. *et al.* Fluorescence lifetime optical projection tomography. *J. Biophotonics* **1**, 390–394 (2008).
53. De Beule, P. *et al.* Rapid hyperspectral fluorescence lifetime imaging. *Microsc. Res. Tech.* **70**, 481–484 (2007).
54. Boens, N. *et al.* Fluorescence lifetime standards for time and frequency domain fluorescence spectroscopy. *Anal. Chem.* **79**, 2137–2149 (2007).
55. Sharman, K.K., Periasamy, A., Asworth, H. & Demas, J.N. Error analysis of the rapid lifetime determination method for double-exponential decays and new windowing schemes. *Anal. Chem.* 71947–71952.
56. Hanley, Q.S. & Clayton, A.H. AB-plot assisted determination of fluorophore mixtures in a fluorescence lifetime microscope using spectra or quenchers. *J. Microsc.* **218**, 62–67 (2005).
57. Redford, G.I. & Clegg, R.M. Polar plot representation for frequency-domain analysis of fluorescence lifetimes. *J. Fluoresc.* **15**, 805–815 (2005).
58. Digman, M.A., Caiolfa, V.R., Zamai, M. & Gratton, E. The phasor approach to fluorescence lifetime imaging analysis. *Biophys. J.* **94**, L14–6 (2008).
59. Verveer, P.J., Squire, A. & Bastiaens, P.I. Global analysis of fluorescence lifetime imaging microscopy data. *Biophys. J.* **78**, 2127–2137 (2000).
60. Pelet, S., Previte, M.J., Laiho, L.H. & So, P.T. A fast global fitting algorithm for fluorescence lifetime imaging microscopy based on image segmentation. *Biophys. J.* **87**, 2807–2817 (2004).
61. Koushik, S.V., Chen, H., Thaler, C., Puhl, H.L., III. & Vogel, S.S. Cerulean, Venus, and VenusY67C FRET reference standards. *Biophys. J.* **91**, L99–L101 (2006).
62. Periasamy, A., Siadat-Pajouh, M., Wodnicki, P., Wang, X.F. & Herman, B. Time-gated fluorescence microscopy for clinical imaging. *Microscopy Anal.* 19–21 (1995).
63. Lundin, K., Blomberg, K., Nordstrom, T. & Lindqvist, C. Development of a time-resolved fluorescence resonance energy transfer assay (cell TR-FRET) for protein detection on intact cells. *Anal. Biochem.* **299**, 92–97 (2001).
64. Zhou, V. *et al.* A time-resolved fluorescence resonance energy transfer-based HTS assay and a surface plasmon resonance-based binding assay for heat shock protein 90 inhibitors. *Anal. Biochem.* **331**, 349–357 (2004).
65. Xu, Z. *et al.* Development of high-throughput TR-FRET and AlphaScreen assays for identification of potent inhibitors of PDK1. *J. Biomol. Screen.* **14**, 1257–1262 (2009).
66. Vogel, S.S., Thaler, C., Blank, P.S. & Koushik, S.V. Time-resolved fluorescence anisotropy. In *FLIM Microscopy in Biology and Medicine* (eds. Periasamy, A. & Clegg, R.M.) 245–288 (CRC Press, 2009).
67. Becker, W. *et al.* Fluorescence lifetime imaging by time-correlated single-photon counting. *Microsc. Res. Tech.* **63**, 58–66 (2004).
68. Stiel, H., Teuchner, K., Paul, A., Leupold, D. & Kochevar, I.E. Quantitative comparison of excited state properties and intensity-dependent photo-sensitization by rose bengal. *J. Photochem. Photobiol. B.* **33**, 245–254 (1996).
69. Periasamy, A. *et al.* Time-resolved fluorescence lifetime imaging microscopy using a picosecond pulsed tunable dye laser system. *Rev. Sci. Instrum.* **67**, 3722–3731 (1996).
70. Becker, W. Recording the instrument response function of a multiphoton FLIM system. *Application Notes* (2007).
71. Rizzo, M.A., Springer, G.H., Granada, B. & Piston, D.W. An improved cyan fluorescent protein variant useful for FRET. *Nat. Biotechnol.* **22**, 445–449 (2004).
72. Ryder, A.G., Glynn, T.J., Przyjalgowski, M. & Szczupak, B. A compact violet diode laser-based fluorescence lifetime microscope. *Journal of Fluorescence* **12**, 177–180 (2002).
73. Thaler, C., Koushik, S.V., Blank, P.S. & Vogel, S.S. Quantitative multiphoton spectral imaging and its use for measuring resonance energy transfer. *Biophys. J.* **89**, 2736–2749 (2005).
74. Nagai, T. *et al.* A variant of yellow fluorescent protein with fast and efficient maturation for cell-biological applications. *Nat. Biotechnol.* **20**, 87–90 (2002).
75. Tang, Q.Q. & Lane, M.D. Activation and centromeric localization of CCAAT/enhancer-binding proteins during the mitotic clonal expansion of adipocyte differentiation. *Genes Dev.* **13**, 2231–2241 (1999).
76. Enwright, J.F. III., Kawecki-Crook, M.A., Voss, T.C., Schaufele, F. & Day, R.N. A PIT-1 homeodomain mutant blocks the intranuclear recruitment of the CCAAT/enhancer binding protein alpha required for prolactin gene transcription. *Mol. Endocrinol.* **17**, 209–222 (2003).
77. Lew, D. *et al.* GHF-1-promoter-targeted immortalization of a somatotrophic progenitor cell results in dwarfism in transgenic mice. *Genes Dev.* **7**, 683–693 (1993).
78. Landschulz, W.H., Johnson, P.F., Adashi, E.Y., Graves, B.J. & McKnight, S.L. Isolation of a recombinant copy of the gene encoding C/EBP. *Genes Dev.* **2**, 786–800 (1988).
79. Chen, Y. & Periasamy, A. Time-correlated single photon counting (TCSPC) FLIM-FRET microscopy for protein localization. In *Molecular Imaging: FRET Microscopy and Spectroscopy* (eds. Periasamy, A. & Day, R.N.) 239–259 (Oxford University Press, 2005).
80. Sun, Y. & Periasamy, A. Additional correction for energy transfer efficiency calculation in filter-based Forster resonance energy transfer microscopy for more accurate results. *J. Biomed. Opt.* **15**, 020513 (2010).